Supporting Information (SI) for:

Morphology and Crystallinity Tuned Luminescent Properties of Lanthanide-Doped YPO_4 Nanoparticles via a Facile Room-Temperature Synthesis

Laishram Peter Singh,§ Loitongbam Thoithoi Singh,§ Aribam Rishikanta Sharma, Thokchom Taru Taru Chanu, Potshangbam Sorodhoni Devi, Konjengbam Jeelina Devi, Ningombam Banshi Devi, W. Rameshwor Singh* and Raju Laishram*

Department of Chemistry, Manipur University, Manipur, 795003, India.

E-mail: dr.rmsingh@yahoo.co.in , rajulaishram007@gmail.com

Table of Contents:

1. Materials and general methods
2. Experimental details
3. Supporting figures
4. Supporting tables

1. Materials and general methods

Materials and Reagents: Yttrium nitrate, $Y(NO_3)_3$, Ammonium dihydrogen phosphate ($NH_4H_2PO_4$), Terbium nitrate, $Tb(NO_3)_3$ and Europium nitrate, $Eu(NO_3)_3$ were purchased from Sigma Aldrich. Citric acid (CA) and Sodium dodecyl sulphate (SDS) were purchased from SRL chemicals. All the chemicals were used without any further purification. Distilled water was used as the only solvent for making all the solutions.

Powder X-ray Diffraction (P-XRD):
Powder X-ray diffraction patterns of samples were recorded using a Bruker D8 ADVANCE ECO P-XRD system with Cu-Kα X-ray source, Ni-filter for low Cu-Kß radiation, and LYNEXYE detector with a step size of 0.02 and a scan step time of 1s per step in the angular range of $2\theta = 10^{o} \leq 2\theta \leq 80^{o}$.

Photoluminescence (PL):
Photoluminescence emission spectra and excitation spectra of the samples were recorded using the Edinburgh FLS980 Fluorimeter instruments equipped with Multichannel Scaling (MCS).

Lifetime and Quantum yield measurement:
Microsecond Lifetimes and Quantum yields (QY) measurements for the samples were performed in Edinburgh FS-5 Fluorometer instruments. For QY measurements, an Integrating Sphere was used.

Transmission Electron Microscopy (TEM):
TEM images were recorded using Field Emission Transmission Electron Microscope (200 kV, JEOL India, Pvt, Ltd. Model :2100F).

Fourier Transform Infrared (FT-IR) measurement:
FT-IR spectra for the nanoparticles and the original capping ligands were recorded using Shimadzu IRAffinity-1S. The original powdered SDS and powdered CA were taken for measurement, and the synthesised nanoparticles were crushed into fine powders using a mortar and pestle to perform the measurements.

2. Experimental details

In a 50 mL beaker, 0.3 M Sodium dodecyl sulphate (SDS) or 0.3M Citric acid (CA) was dissolved in 10 mL of water. To it, 0.3 M $Y(NO_3)_3$, 0.3 M $NH_4H_2PO_4$ and 10% $Tb(NO_3)_3$ (0.3 M) were added. The mixture was stirred at ~700 rpm at room temperature for ~1 hr to get a state of homogeneity. The white precipitate so obtained was separated by centrifugation at approximately 4500 rpm for 5 minutes, followed by continuous washing 3 times with distilled water and twice with acetone. The prepared material was dried at room temperature for two days.

For red emissive nanoparticles, 10% $Eu(NO_3)_3$ (0.3 M) was used instead of $Tb(NO_3)_3$. A 7:3 molar ratio of Tb^{3+}/Eu^{3+} was used for obtaining yellow emissive nanoparticles for SDS and CA-capped YPO_4 nanoparticles.

Supporting Figures

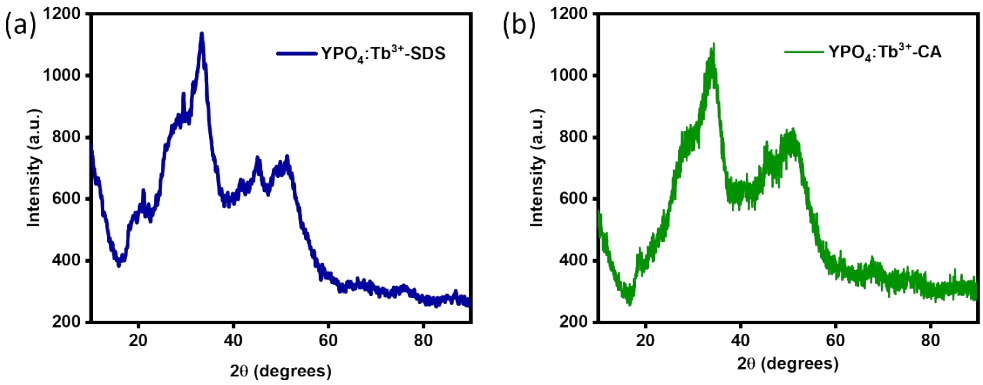

Figure S1. pXRD spectra of (a) YPO_4:Tb^{3+}-SDS and (b) YPO_4:Tb^{3+}-CA nanoparticles.

Note: A broad peak of the XRD patterns is observed in both cases. This demonstrates the morphological changes of the materials that occurred in the presence of the capping agents, SDS and CA.

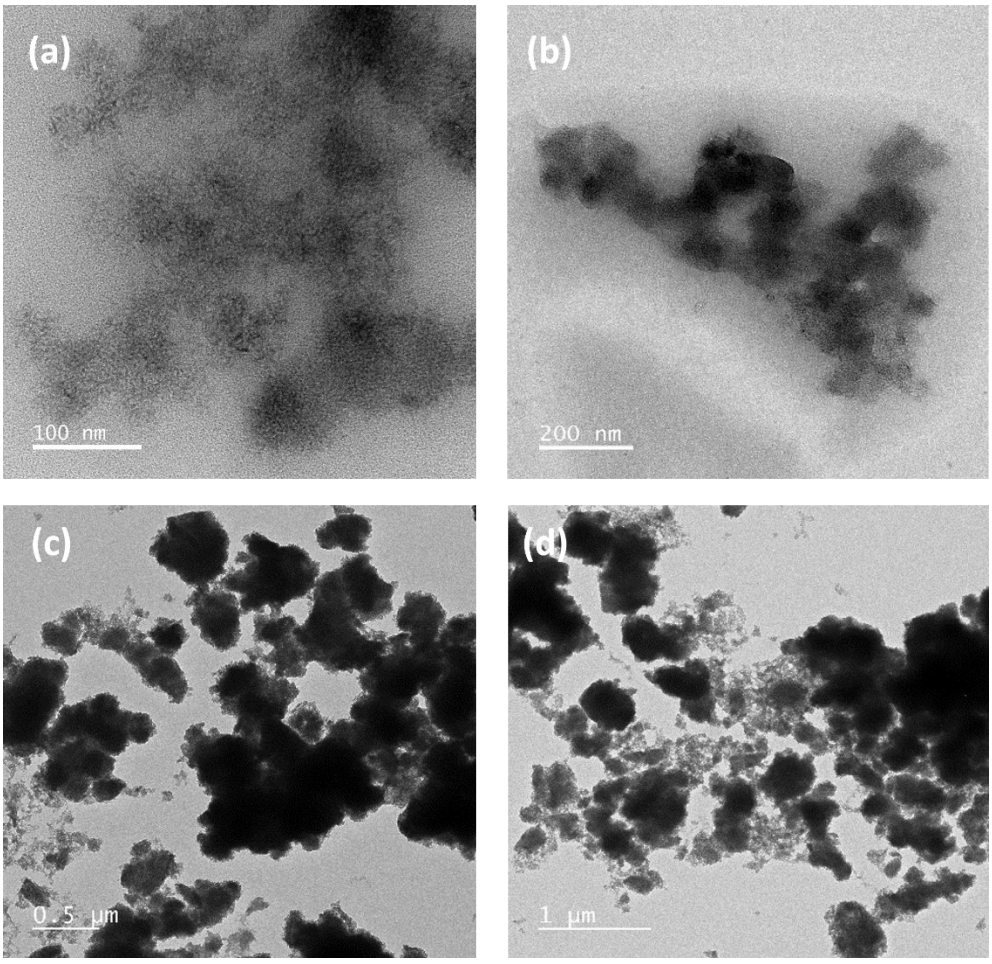

Figure S2. TEM images of (a)-(b) YPO_4:Tb^{3+}-SDS and (c)-(d) YPO_4:Tb^{3+}-CA nanoparticles.

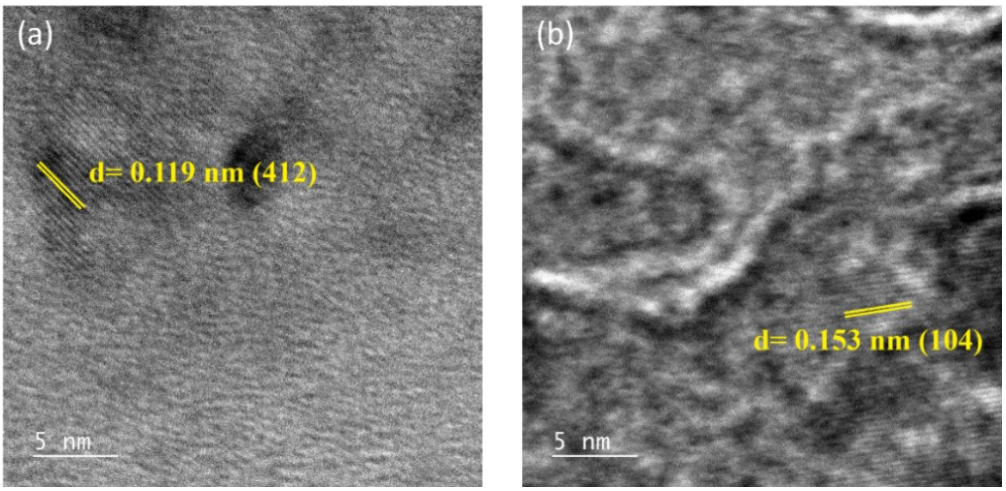

Figure S3. HRTEM images of (a) YPO_4:Tb^{3+}-SDS and (b) YPO_4:Tb^{3+}-CA nanoparticles. YPO_4:Tb^{3+}-SDS and YPO_4:Tb^{3+}-CA showed the lattice fringes with a lattice spacing of 0.119 nm and 0.153 nm, respectively, which correspond to the 412 and 104 planes of the hexagonal phase YPO_4 nanoparticles (JCPDS file no-42-0082).

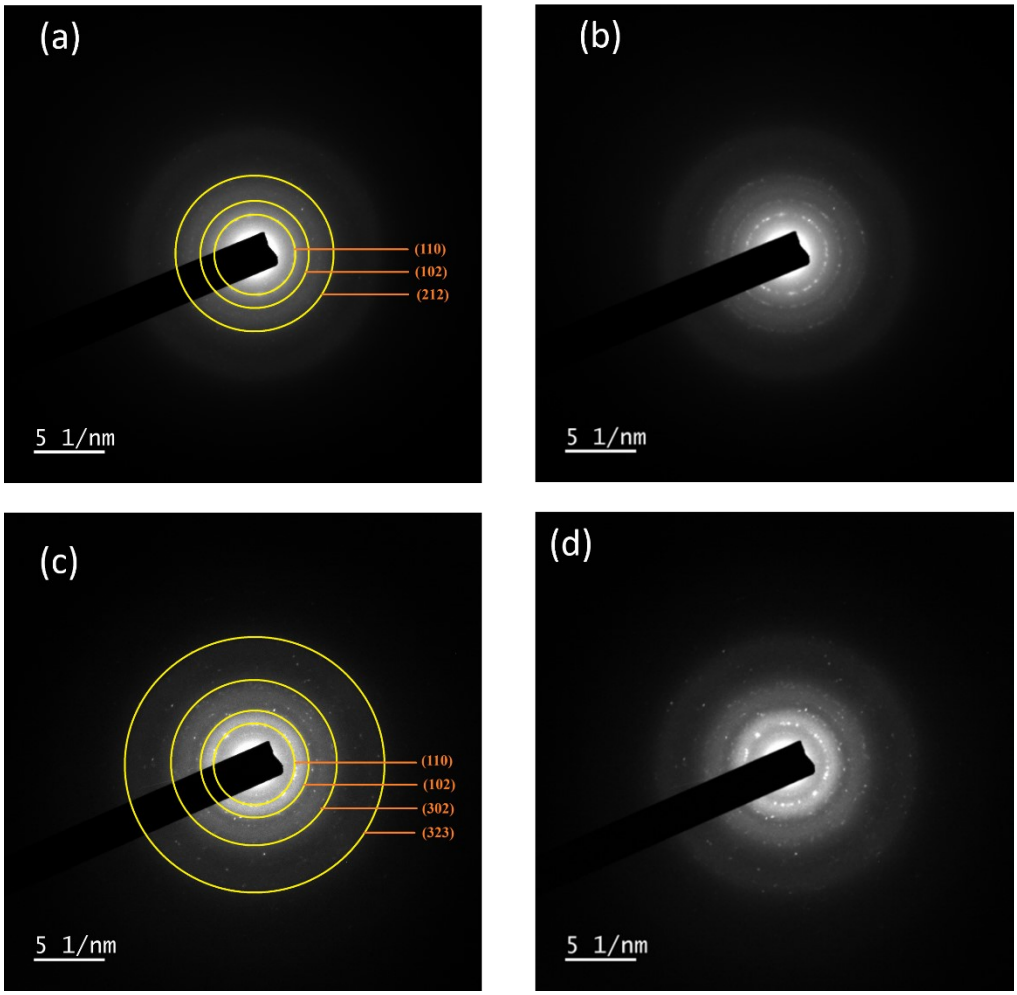

Figure S4. SAED patterns of (a) YPO_4:Tb^{3+}-SDS, (b) YPO_4:Tb^{3+}-SDS nanoparticles without rings. For YPO_4:Tb^{3+}-SDS, the derived d-spacing corresponds to [(110), (102) and (212)] planes of the hexagonal phase YPO_4 nanoparticles. SAED patterns of (c) YPO_4:Tb^{3+}-CA nanoparticles, and (b) YPO_4:Tb^{3+}-CA nanoparticles without rings. For YPO_4:Tb^{3+}-CA nanoparticle, the d-spacing also corresponds to different planes [(110), (102), (302), and (323)] of hexagonal YPO_4 nanoparticles. (JCPDS file no-42-0082).

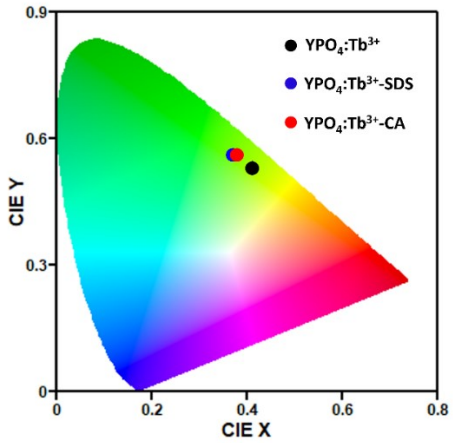

Figure S5. CIE 1931 Plot for $YPO_4:Tb^{3+}$, $YPO_4:Tb^{3+}$-SDS and $YPO_4:Tb^{3+}$-CA nanoparticles with CIE coordinates of (0.41, 0.53), (0.37, 0.56) and (0.38, 0.56), respectively, derived from their respective emission data.

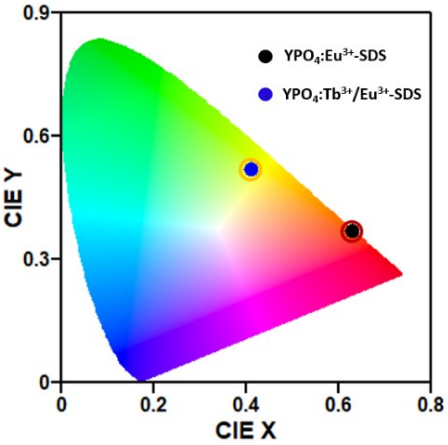

Figure S6. CIE 1931 Plot for $YPO_4:Eu^{3+}$-SDS and $YPO_4:Tb^{3+/}Eu^{3+}$-SDS nanoparticles with CIE coordinates of (0.63, 0.37) and (0.41, 0.52), respectively, derived from their respective emission data.

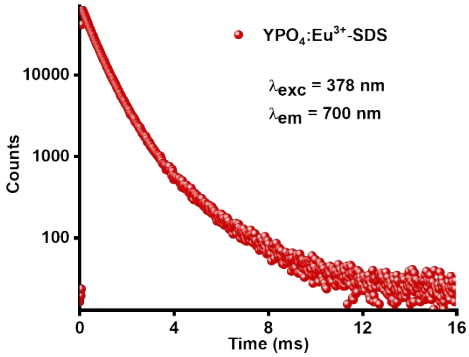

Figure S7. Lifetime decay plot for Eu^{3+} in $YPO_4:Eu^{3+}$-SDS at an excitation and emission wavelengths of 378 nm and 700 nm, respectively.

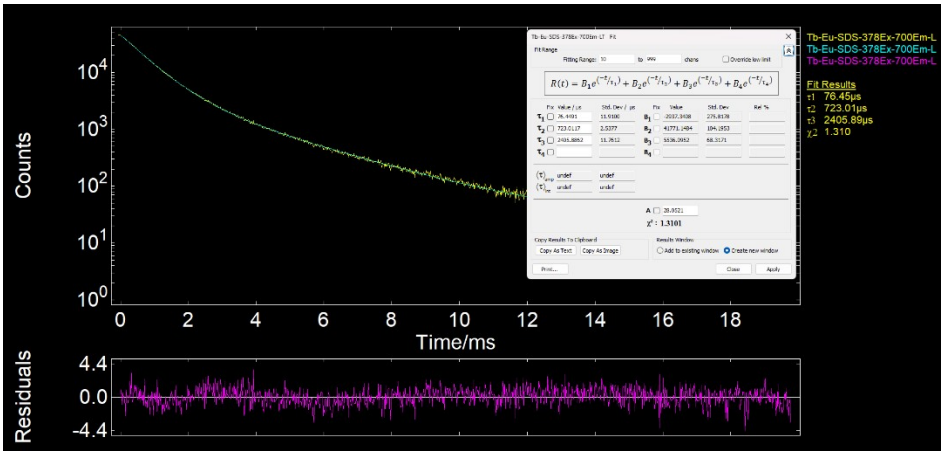

Figure S8. Fitted Lifetime decay plot for Eu^{3+} in YPO_4:Tb^{3+}/Eu^{3+}-SDS at an excitation and emission wavelengths of 378 nm and 700 nm, respectively.

Note: A negative pre-exponential value is observed in the fitted data of the Eu^{3+}, indicating its rise time due to the energy transfer from Tb^{3+}.

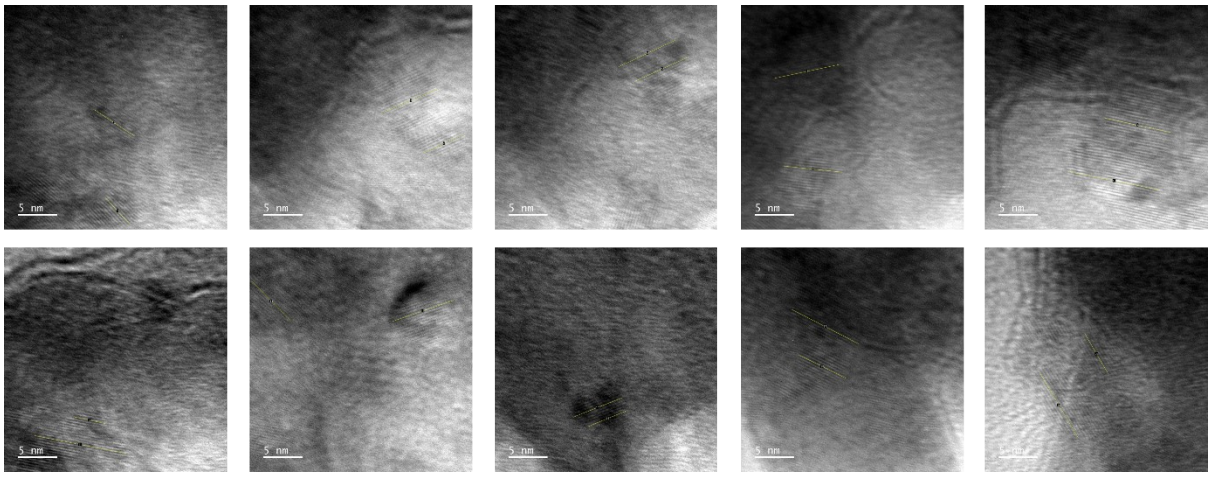

Figure S9. Representative HRTEM images of YPO_4:Tb^{3+}-SDS nanoparticles for determining the average fringe length (Scale bar = 5 nm). The selected fringes are marked with yellow lines.

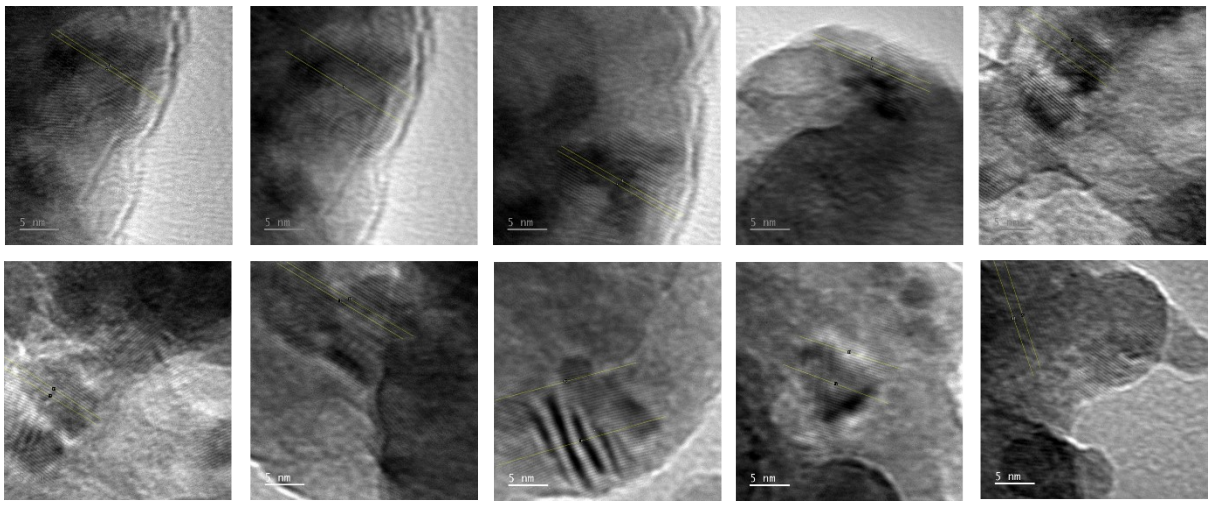

Figure S10. Representative HRTEM images of YPO_4:Tb^{3+}-CA nanoparticles for determining the fringe length (Scale bar = 5 nm). The selected fringes are marked with yellow lines.

Note: The average fringe lengths for YTS and YTC were 9.14±2.8 nm and 15.72±2.3 nm, respectively. 10 representative images each for YTS and YTC are depicted in Fig. S9 and Fig. S10, respectively.

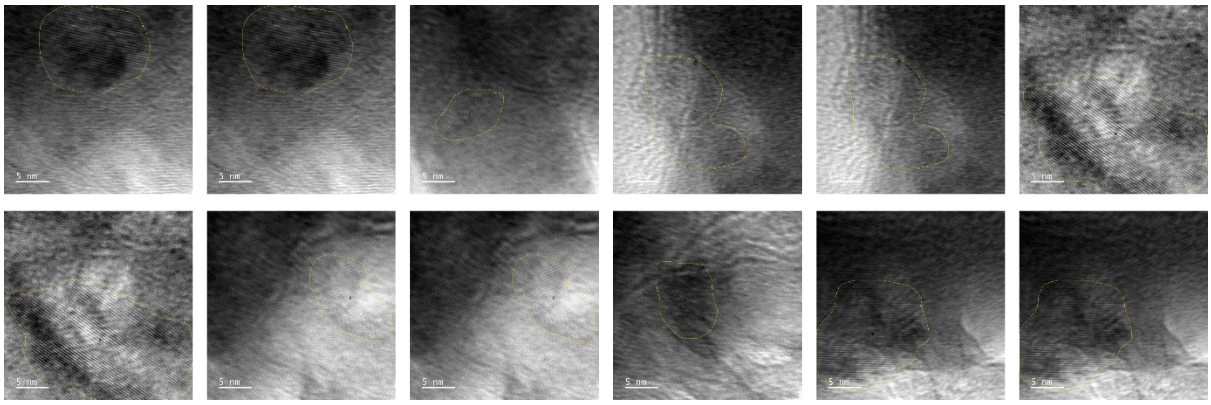

Figure S11. Representative HRTEM images of YPO_4:Tb^{3+}-SDS nanoparticles for determining the average equivalent diameter of the nanoparticle by selecting the areas of clear and continuous fringes distribution in the image for calculating the crystallite size (Scale bar = 5 nm). The selected areas are marked in yellow encircles.

Note: After setting the scale in ImageJ, we drew and measured the fringe distribution area in HRTEM images using freehand selections.

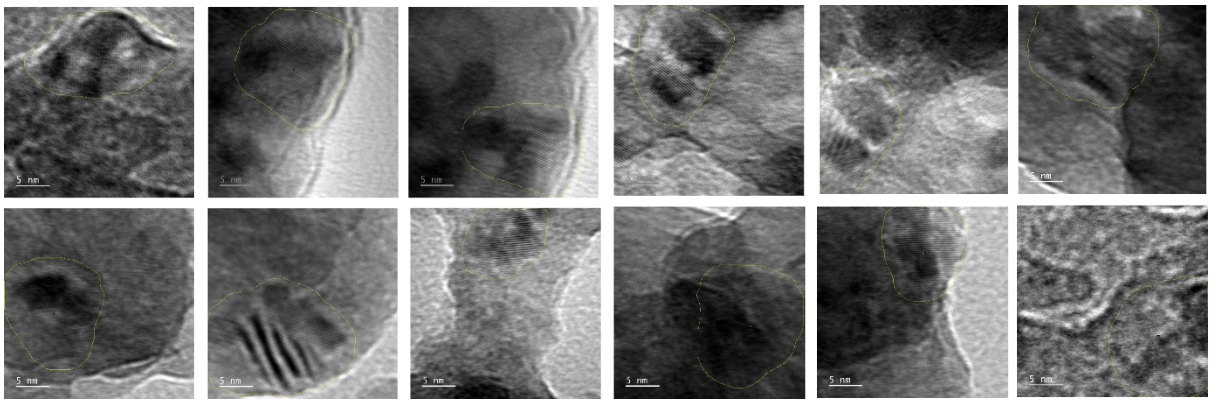

Figure S12. Representative HRTEM images of YPO_4:Tb^{3+}-CA nanoparticles for determining the average equivalent diameter of the nanoparticle by selecting the areas of clear and continuous fringes distribution in the image for calculating the crystallite size (Scale bar = 5 nm). The selected areas are marked in yellow encircles.

Note: As shown in the bar diagram Fig. 6e-f, the YPO_4:Tb^{3+}-CA nanoparticles have a larger average crystallite (~16 nm in diameter) size than the YPO_4:Tb^{3+}-SDS nanoparticles (~11 nm in diameter), indicating that the YPO_4:Tb^{3+}-CA nanoparticles have higher crystallinity than the YPO_4:Tb^{3+}-SDS nanoparticles.

The average equivalent diameters were calculated using W. Pabst and E. Gregorová's formula:[1]

$$\text{Average equivalent circular diameter, } D_{av} = 2x\sqrt{\frac{A}{\pi}}$$, where A is the average area of the particles.

40 HRTEM images each for YPO_4:Tb^{3+}-SDS and YPO_4:Tb^{3+}-CA were taken into consideration for finding out their respective average areas using ImageJ software, out of which 12 representative images for each nanoparticle are given in Fig. S11 and Fig. S12.

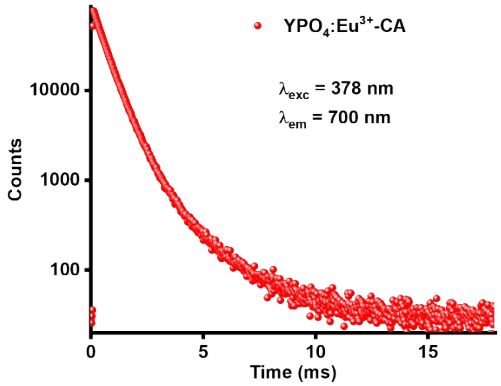

Figure S13. Lifetime decay plot for Eu^{3+} in YPO_4:Eu^{3+}-CA at an excitation and emission wavelengths of 378 nm and 700 nm, respectively.

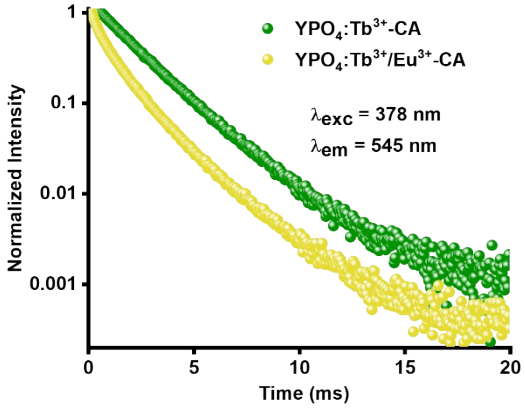

Figure S14. Lifetime decay plot for Tb^{3+} ion in YPO_4:Tb^{3+}-CA and YPO_4:Tb^{3+}/Eu^{3+}-CA at an excitation and emission wavelengths of 378 nm and 545 nm, respectively.

Note: The lifetime of Tb^{3+} is decreased in the presence of the Eu^{3+} ion, indicating that Tb^{3+} acts as the donor for the energy transfer to the Eu^{3+} ion.

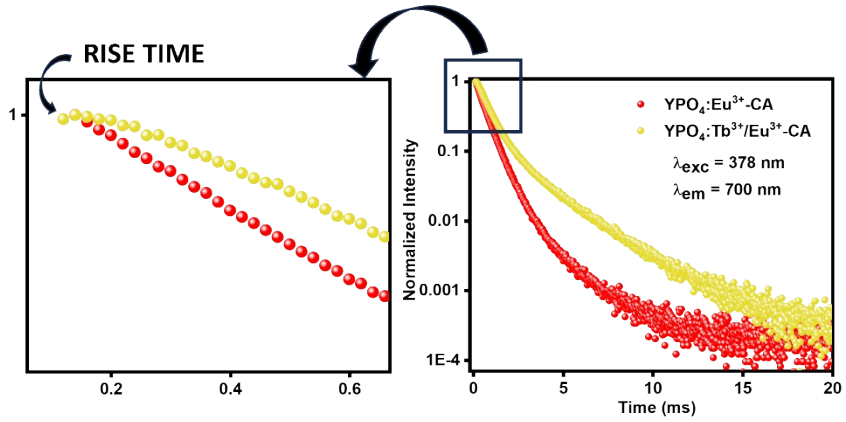

Figure S15. Lifetime decay plot for Eu^{3+} ion in YPO_4:Eu^{3+}-CA and YPO_4:Tb^{3+}/Eu^{3+}-CA at an excitation and emission wavelengths of 378 nm and 700 nm, respectively.

Note: The rise time is clearly evident in the lifetime decay plot of the acceptor (Eu^{3+}) in the mixed Tb^{3+}/Eu^{3+} system, providing a strong mechanistic insight into the energy transfer process.

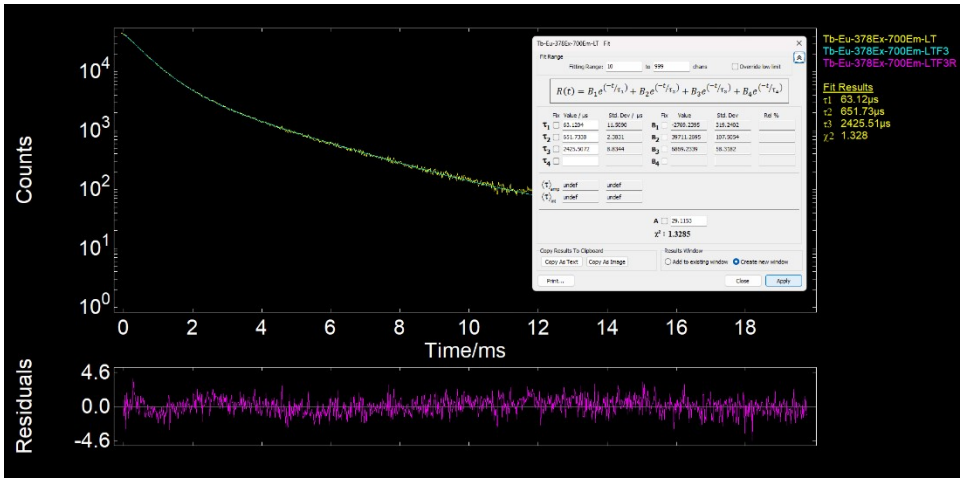

Figure S16. Fitted Lifetime decay plot for Eu^{3+} in YPO_4:Tb^{3+}/Eu^{3+}-CA at an excitation and emission wavelengths of 378 nm and 700 nm, respectively.

3. Supporting tables

Table S1. Quantum yields (**Φ**) for different samples.

SL.No.	Sample	Φ (%)
1	**YPO_4:Tb^{3+}-SDS**	7.0
2	**YPO_4:Eu^{3+}-SDS**	2.9
3	**YPO_4:Tb^{3+}/Eu-SDS**	3.3
4	**YPO_4:Tb^{3+}-CA**	16.8
5	**YPO_4:Eu^{3+}-CA**	9.9
6	**YPO_4:Tb^{3+}/Eu-CA**	11.6

Table S2. Fluorescence Lifetimes of Tb^{3+} ions and Eu^{3+} ions at an excitation and emission wavelengths of 378 nm and 545 nm (Tb^{3+}) and 700 nm (Eu^{3+}), respectively, for different samples.

SL. No.	Species	Sample [λ_{exc} = 378 nm, λ_{em} = 545 nm (Tb^{3+}), 700 nm (Eu^{3+})]	τ_1 (ms)	Relative component B_1 (%)	τ_2 (ms)	Relative Component B_2 (%)	τ_3 (ms)	Relative Component B_3 (%)	τ_{av} (ms)	χ^2
1	**Tb^{3+}**	**YPO_4:Tb^{3+}-SDS**	0.56	1.68	1.60	70.34	2.63	27.98	1.87	1.17
2	**Eu^{3+}**	**YPO_4:Eu^{3+}-SDS**	0.36	13.72	0.69	71.65	1.95	14.64	0.83	1.27
3	**Tb^{3+}**	**YPO_4:Tb^{3+}/Eu^{3+}-SDS**	0.28	4.37	1.08	30.43	1.99	65.20	1.63	1.03
4	**Eu^{3+}**	**YPO_4:Tb^{3+}/Eu^{3+}-SDS**	0.076		0.72		2.40			1.31
5	**Tb^{3+}**	**YPO_4:Tb^{3+}-CA**	0.27	0.19	1.63	61.18	2.63	38.63	2.01	1.05
6	**Eu^{3+}**	**YPO_4:Eu^{3+}-CA**	0.42	26.61	0.68	64.84	2.02	8.56	0.72	1.16
7	**Tb^{3+}**	**YPO_4: Tb^{3+}/Eu^{3+}-CA**	0.30	7.59	1.12	55.58	2.38	36.83	1.52	1.22
8	**Eu^{3+}**	**YPO_4: Tb^{3+}/Eu^{3+}-CA**	0.063		0.65		2.42			1.32

Table S3. Radiative decay constant (k_r) and non-radiative decay constant (k_{nr}) values for different samples with respect to their quantum yields (**Φ**) and average lifetimes (τ_{av}).

SL.No.	Sample	Φ (%)	τ_{av} (ms)	k_r	k_{nr}	k_{nr}/k_r
1	**$YPO_4:Tb^{3+}$-SDS**	7.0	1.87	0.04	0.50	12.5
2	**$YPO_4:Eu^{3+}$-SDS**	2.9	0.83	0.03	1.17	39
3	**$YPO_4:Tb^{3+}$/Eu-SDS**	3.3	1.63	0.02	0.59	29.5
4	**$YPO_4:Tb^{3+}$-CA**	16.8	2.01	0.08	0.41	5.12
5	**$YPO_4:Eu^{3+}$-CA**	9.9	0.72	0.14	1.25	8.93
6	**$YPO_4:Tb^{3+}$/Eu-CA**	11.6	1.52	0.07	0.58	8.28

References:

1. W. Pabst and E. J. I. P. Gregorova, *ICT Prague*, 2007, **122**, 122.